Conjugate free convection along a thin vertical plate with internal nonuniform heat generation in a porous medium

F. Méndez, C. Treviño, I. Pop, A. Liñán

List of symbols

A	constant in Eq. (41)
B	constant defined in Eq. (37)
$C_1(s)$	function defined in Eq. (47)
C_s	specific heat of the strip
f	non-dimensional reduced stream function defined in Eq. (9)
g	acceleration due to gravity
h	thickness of the strip
k	thermal conductivity
K	permeability of the porous medium
L	length of the strip
m_c	total mass flow rate defined in Eq. (12)
$m_r(s)$	non-dimensional reduced mass flow rate of the fluid
Ra	modified Rayleigh number based on ΔT
Ra_c	modified Rayleigh number based on ΔT_c defined in Eq. (10)
s	parameter associated with the distribution of the internal heat source in the strip
S	internal heat source
T	temperature
T_∞	ambient temperature
u, v	velocity components along x and y-axes
z	non-dimensional normal coordinate of the strip defined in Eq. (9)

Greek symbols

α	heat conduction parameter
α_f	thermal diffusivity of the fluid
α_s	thermal diffusivity of the strip
β	coefficient of thermal expansion
δ	boundary-layer thickness
ΔT	temperature difference across the fluid layer
ΔT_c	characteristic temperature difference defined in Eq. (11)
ϕ	non-dimensional internal heat generation function defined in Eq. (9)
ϵ	aspect ratio of the strip
η	non-similarity variable defined in Eq. (9)
ν	kinematic viscosity
ρ	density
ξ	non-similarity variable defined in Eq. (31)
θ	non-dimensional temperature function
χ	non-dimensional longitudinal coordinate defined in Eq. (9)
ψ	dimensional stream function

Subscripts

f	fluid
s	solid strip
w	condition on the strip
∞	ambient condition

Superscript

$\bar{}$	averaged non-dimensional temperature

Abstract The steady state heat transfer characteristics of a thin vertical strip with internal heat generation placed in a porous medium is studied in this work. The non-dimensional temperature distribution in the strip is obtained as a function of the intensity and distribution of the internal heat sources. Both the thermally thin as the thick wall approximations are considered in this paper. The mass flow rate of fluid induced by heating the strip decreases as the longitudinal heat conduction effects along the strip decreases.

1 Introduction

Transport processes in porous media are encountered in a broad range of scientific and engineering problems associated with the petroleum and geothermal industries, fibre and granular insulation materials, storage of radioactive nuclear waste materials, packed-bed chemical reactors and transpiration cooling. Literature concerning convective flow in porous media is abundant. Representative studies in this area may be found in the recent books by Ingham and Pop [1], Nield and Bejan [2] and Vafai [3]. It is well-established that convective heat transfer depends on the

form of the thermal boundary conditions imposed, with it being usual to take either a prescribed temperature or a prescribed heat flux on the bounding surface. However, there are many problems of practical importance where the surface conditions cannot be specified so simply and these then depend strongly on the convective heat transfer within the bounding solid wall. In these situations free or mixed convection must then be studied as a mixed problem, termed a conjugate problem, where there is an interaction between the convective flow in the fluid and the heat conduction within the solid wall. In particular, papers by Bejan and Anderson [4], Vynnycky and Kimura [5, 6], Pop and Merkin [7], Pop et al. [8], Lesnic et al. [9], Higuera and Pop [10], Higuera [11] and Shu and Pop [12–14] have elucidated the effects of the appropriate conjugate parameters on the heat conduction in the solid walls coupled with natural or mixed convection flows adjacent to vertical and horizontal flat surfaces embedded in a fluid-saturated porous medium. The early theoretical work of conjugate free convection in porous media has been recently reviewed by Kimura et al. [15]. However, in most of these studies the authors have provided analytical or computed solutions to the governing equations by assuming a thin heated plate so that conduction within the plate is one-dimensional. In view of this observation, conjugate heat transfer for the most general case, when the heated vertical plate is assumed to be of both finite thickness and length, corresponding to the presence of axial conduction effects, has yet to be treated fully. The present paper considers in detail the temperature distribution in a thin vertical flat plate (strip) with non-uniform internal heat generation and embedded in a fluid-saturated porous medium. We tackle this topic using both numerical and analytical methods. The non-dimensional temperature distribution in the solid plate is obtained as a function of the following parameters: (a) the intensity and distribution of the internal heat sources, (b) the aspect ratio of the plate and (c) the longitudinal heat conductance of the plate. The problem and solution method is analogous to that of Méndez and Treviño [16] for a thin vertical plate immersed in a viscous (non-porous) incompressible fluid.

2
Basic equations

The physical model and a suitable coordinate system are given in Fig. 1. We consider the free convection boundary-layer flow induced by a vertical heated conducting strip of length L and thickness h, which is totally embedded in a vertical flat plate and placed in a fluid-saturated porous medium. It is assumed that the right face of the strip is at the temperature T_∞, whilst the left upper and lower walls are supposed to be adiabatic. This condition is satisfied if the ratio of the thermal conductivity of the flat plate to the thermal conductivity of the strip is much smaller than unity, see for example Sathe and Joshi [17]. Under the Darcy-Boussinesq and boundary-layer approximations, the free convection flow is described by the equation of continuity

$$\frac{\partial u}{\partial x}+\frac{\partial v}{\partial y}=0 \tag{1}$$

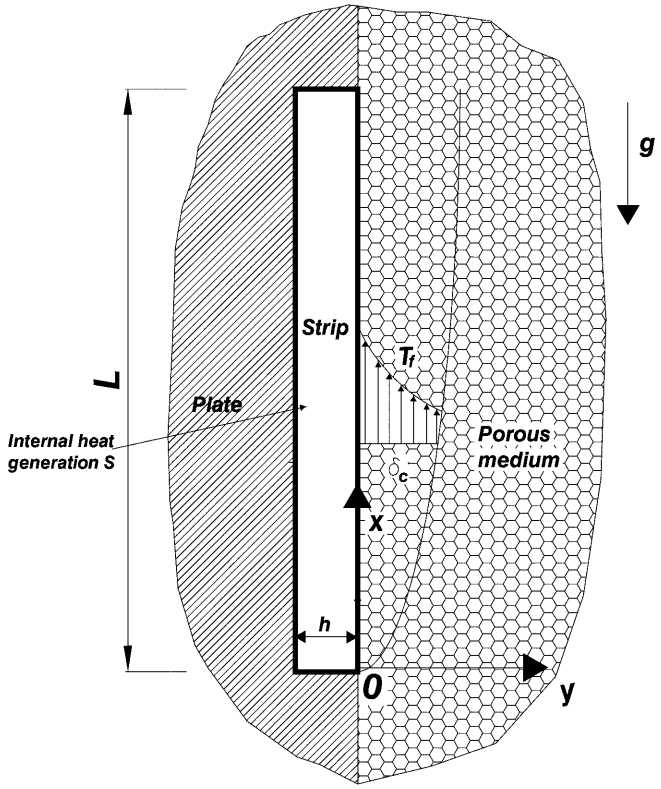

Fig. 1. Physical model and the coordinate system

Darcy's law

$$u=\frac{gK\beta_f}{\nu_f}(T_f-T_\infty) \tag{2}$$

the equation of energy in the fluid-porous medium

$$u\frac{\partial T_f}{\partial x}+v\frac{\partial T_f}{\partial y}=\alpha_f\frac{\partial^2 T_f}{\partial y^2} \tag{3}$$

and the equation of heat transfer inside the solid plate

$$\alpha_s\left(\frac{\partial^2 T_s}{\partial x^2}+\frac{\partial^2 T_s}{\partial y^2}\right)+\frac{S}{\rho_s C_s}=0 \tag{4}$$

where the physical quantities in these equations are described in the Nomenclature. Equations (1)–(4) are subject to the following boundary conditions:

$$v=0,\ T_f=T_s,\ k_f\frac{\partial T_f}{\partial y}=k_s\frac{\partial T_s}{\partial y}\ \text{ on } y=z=0 \tag{5}$$

$$\frac{\partial T_s}{\partial y}=0\quad \text{at } y=-h \tag{6}$$

$$\frac{\partial T_s}{\partial x}=0\quad \text{at } x=0 \text{ and } x=L \tag{7}$$

$$u\to 0,\quad T_f\to T_\infty \text{ as } y\to\infty\ . \tag{8}$$

We introduce now the following non-dimensional variables

$$\chi=\frac{x}{L},\ \eta=\frac{\mathrm{Ra}_c^{1/2}}{\chi^{1/2}}\frac{y}{L},\ z=\frac{y}{h},\ f=\frac{\psi}{\alpha_f \mathrm{Ra}_c^{1/2}\chi^{1/2}}$$
$$\theta_f=\frac{T_f-T_\infty}{\Delta T_c},\ \theta_s=\frac{T_s-T_\infty}{\Delta T_c},\ \phi=\frac{S}{\bar{S}} \tag{9}$$

where ΔT_c is the characteristic temperature to be defined later, ψ is the stream function which is defined as $u = \partial\psi/\partial y$ and $v = -\partial\psi/\partial x$, Ra_c is the modified Rayleigh number for the porous medium and $\bar{S}$ is the averaged volumetric heat production term which are defined as

$$Ra_c = \frac{gK\beta_f \Delta T_c L}{\alpha_f \nu_f}, \quad \bar{S} = \frac{1}{L}\int_0^L S\,dx \ . \tag{10}$$

An order of magnitude analysis shows that the characteristic velocity in the fluid is $u_c \sim Ra_c \alpha_f / L$. Assuming large values of Ra_c compared with unity, the boundary layer thickness is of order $\delta_c \sim L/Ra_c^{1/2}$. On the other hand, using the fact that the total heat production in the solid $\bar{S}hL$ is of same order than the total heat transfer to the fluid $k_f \Delta T_c Ra_c^{1/2}$, then it is easy to show that the characteristic temperature difference must be of order

$$\Delta T_c = \frac{\Delta T^*}{Ra^{*1/3}} \ . \tag{11}$$

Here ΔT^* is related to the heat generated internally and is defined by $\Delta T^* = \bar{S}hL/k_f$. The Rayleigh number Ra^* is given by $Ra^* = Ra(\Delta T^*)$, where $Ra = gK\beta\Delta TL/\alpha_f \nu$ is the Rayleigh number for the porous medium, with ΔT being the actual temperature difference across the fluid layer, which is in fact to be obtained from the analysis. Using (11), we then have $Ra_c = Ra^{*2/3}$. Therefore, the total mass flow rate m_c is of the order

$$m_c \sim Ra^{*1/3} \rho_f \alpha_f \sim \left(\frac{gK\beta_f \alpha_f^2}{\nu_f k_f}\right)^{1/3} \rho_f (\bar{S}h)^{1/3} L^{4/3} \ . \tag{12}$$

Similarly, the order of magnitude of the transversal, ΔT_{sh}, and longitudinal, ΔT_{sL}, characteristic temperature differences in the solid plate related to the characteristic temperature difference, ΔT_c, are given by

$$\frac{\Delta T_{sh}}{\Delta T_c} \sim \left(1 + \frac{\varepsilon^2}{\alpha}\right)^{-1} \quad \text{and} \quad \frac{\Delta T_{sL}}{\Delta T_c} \sim (\alpha + \varepsilon^2)^{-1} \tag{13}$$

where $\alpha = (k_s/k_f)(h/L)Ra_c^{-1/2}$ and $\varepsilon = h/L$. For values of $\alpha \gg \varepsilon^2$, the temperature variation in the transversal direction in the solid is negligible small compared with the overall temperature difference and this is called thermally thin wall regime. In this limit the longitudinal temperature variation compared with ΔT_c is of order $1/\alpha$.

Substituting (9) into Eq. (2) gives $\theta_f = \partial f/\partial\eta$ and using this relation, Eq. (3) becomes

$$\frac{\partial^3 f}{\partial\eta^3} + \frac{1}{2} f \frac{\partial^2 f}{\partial\eta^2} = \chi\left(\frac{\partial f}{\partial\eta}\frac{\partial^2 f}{\partial\chi\partial\eta} - \frac{\partial f}{\partial\chi}\frac{\partial^2 f}{\partial\eta^2}\right) \tag{14}$$

for the fluid-saturated porous medium and

$$\alpha\frac{\partial^2\theta_s}{\partial\chi^2} + \frac{\alpha}{\varepsilon^2}\frac{\partial^2\theta_s}{\partial z^2} + \phi = 0 \tag{15}$$

for the strip. The boundary conditions (5) to (8) become

$$f = \frac{\partial f}{\partial\eta} - \theta_s = \frac{\partial\theta_s}{\partial z} - \frac{\varepsilon^2}{\alpha\chi^{1/2}}\frac{\partial^2 f}{\partial\eta^2} = 0 \quad \text{at } \eta = z = 0 \tag{16}$$

$$\frac{\partial\theta_s}{\partial z} = 0 \quad \text{at } z = -1 \tag{17}$$

$$\frac{\partial\theta_s}{\partial\chi} = 0 \quad \text{for } \chi = 0 \text{ and } \chi = 1 \tag{18}$$

$$\frac{\partial f}{\partial\eta} \to 0 \quad \text{as } \eta \to \infty \ . \tag{19}$$

Thus, we have a set of two partial differential equations subject to the boundary conditions (16) to (19) one being parabolic, Eq. (14), and the other one, Eq. (15), being elliptic, which govern the development of the free convection boundary-layer flow near the strip. This system can be solved numerically and this, together with an asymptotic analysis for both thermally thin wall regime (the temperature variations across the strip is negligibly small) and thermal thick wall regime (strong temperature variations in the axial and transversal directions of the strip). The solution of the problem should provide the temperature of the strip $\theta_s = \theta_s(\alpha, \varepsilon, \phi, \chi, z)$.

Here, taking advantage of the fact that ε^2 is very small compared with unity in general, we classify the solutions according to the value of α. For large values of α/ε^2 ($\gg 1$) the transversal temperature variation in the plate is very small and therefore the plate temperature θ_s can be assumed to be a function of the longitudinal coordinate χ only. It is to be noted that neglecting the transversal temperature variation does not mean neglecting the transversal temperature gradient, which always is important and should be retained in the analysis. In the following section we present numerical solutions of the corresponding problem for $\alpha = O(1)$ and analyze the limits of large and small values of α using both asymptotic and numerical techniques. The temperature variation across the plate must be taken into account for $\alpha/\varepsilon^2 = O(1)$, but the longitudinal heat conduction is then negligibly small (except in small regions close to the edges of the plate), leading to a linear variation of the temperature across the plate.

3
Thermally thin wall regime

For large values of α/ε^2 ($\gg$1), the non-dimensional transversal temperature variation in the plate is very small, namely, of order ε^2/α ($\ll$1). Integrating the energy equation (15) across the non-dimensional z coordinate and applying the suitable boundary and compatibility conditions (16) and (17), we obtain

$$\alpha\frac{d^2\theta_s}{d\chi^2} = -\phi - \frac{1}{\chi^{1/2}}\left.\frac{\partial^2 f}{\partial\eta^2}\right|_{\eta=0} \ . \tag{20}$$

This equation must be solved with the adiabatic conditions (18) of the strip and the set of equations given by (14), (16) and (19). In this section, we develop the numerical and asymptotic solutions for large values of α.

3.1
Asymptotic limit $\alpha \to \infty$

The asymptotic solution of the problem for large values of α ($\gg$1) is very important and is applicable to many practical cases of metallic plates in air or water (see Cordova

and Treviño [18]). In this case the non-dimensional temperature of the plate, θ_s, changes very little in the longitudinal direction, as suggested by the analysis of Méndez and Treviño [16]. In fact, this change is of order α^{-1} as shown by the estimation of the order of magnitude of θ_s. The asymptotic solution for the temperature of the plate and the reduced stream function of the fluid is regular and is to be analyzed using α^{-1} as the small expansion parameter. In this limit, the solution is sought as power series expansions of the form

$$\theta_s = \sum_{j=0}^{\infty} \frac{1}{\alpha^j} \theta_{sj}(\chi) \tag{21}$$

and

$$f = f_0(\eta) + \sum_{j=1}^{\infty} \frac{1}{\alpha^j} f_j(\chi, \eta) \ . \tag{22}$$

Substituting these expansions into the non-dimensional governing Eqs. (20) and (14), and the corresponding boundary conditions (16)–(19), and we limit our analysis up to terms of order α^{-2} for the solid plate and up to terms of order α^{-1} for the fluid-porous medium, we obtain the following set of equations

Solid:

$$\frac{d^2\theta_{s0}}{d\chi^2} = 0 \tag{23}$$

$$\frac{d^2\theta_{s1}}{d\chi^2} = -\phi - \frac{1}{\chi^{1/2}} \frac{d^2 f_0}{d\eta^2}\bigg|_{\eta=0} \tag{24}$$

$$\frac{d^2\theta_{sj}}{d\chi^2} = -\frac{1}{\chi^{1/2}} \frac{\partial^2 f_{j-1}}{\partial \eta^2}\bigg|_{\eta=0} \quad \text{for } j = 2, 3, \ldots \tag{25}$$

with the adiabatic boundary conditions

$$\frac{d\theta_{sj}}{d\chi} = 0 \quad \text{at } \chi = 0 \text{ and } \chi = 1, \quad \text{for } j = 0, 1, \ldots \tag{26}$$

Fluid:

$$\frac{d^3 f_0}{d\eta^3} + \frac{1}{2} f_0 \frac{d^2 f_0}{d\eta^2} = 0 \tag{27}$$

$$\frac{\partial^3 f_1}{\partial \eta^3} + \frac{1}{2}\left(f_0 \frac{\partial^2 f_1}{\partial \eta^2} + \frac{d^2 f_0}{d\eta^2} f_1 \right) - \chi \left[\frac{df_0}{d\eta} \frac{\partial^2 f_1}{\partial \chi \, \partial \eta} - \frac{d^2 f_0}{d\eta^2} \frac{\partial f_1}{\partial \chi} \right] = 0 \tag{28}$$

with the boundary conditions

$$f_j = \frac{\partial f_j}{\partial \eta} - \theta_{sj} = 0 \quad \text{on } \eta = 0 \tag{29}$$

and

$$\frac{\partial f_j}{\partial \eta} = 0 \quad \text{as } \eta \to \infty \tag{30}$$

for $j = 0, 1, 2, \ldots$. In order to simplify the set of Eqs. (23)–(30), we use the invariance of the above boundary layer equations, under the group of transformations $\theta_s \Longrightarrow B\theta_s$, $\eta \Longrightarrow B^{-1/2}\eta$ and $f \Longrightarrow B^{1/2} f$, noting that the solution of Eq. (23) with the adiabatic boundary conditions (26) is trivial, giving $\theta_{s0} = B$ = constant, which has to be obtained by solving Eqs. (24) and (27), with the above given transformations. Therefore, we introduce the new variables

$$\xi = (\theta_{s0})^{1/2} \eta, \quad g_0 = \frac{f_0}{(\theta_{s0})^{1/2}} \tag{31}$$

to reduce Eq. (27) to

$$\frac{d^3 g_0}{d\xi^3} + \frac{1}{2} g_0 \frac{d^2 g_0}{d\xi^2} = 0 \tag{32}$$

with the boundary conditions

$$g_0(0) = \frac{dg_0}{d\xi}\bigg|_{\xi=0} - 1 = 0 \quad \text{and} \quad \frac{dg_0}{d\xi}\bigg|_{\xi\to\infty} = 0 \ . \tag{33}$$

The solution of Eqs. (32) and (33) can be found elsewhere [2 or 19], corresponding to the classical problem of a solid wall with uniform temperature. The non-dimensional temperature gradient at the wall is then given by

$$\frac{d^2 g_0}{d\xi^2}\bigg|_{\xi=0} = -G_0 = -0.444 \quad \text{or} \quad \frac{d^2 f_0}{d\eta^2}\bigg|_{\eta=0} = -\frac{1}{2} \ . \tag{34}$$

With the aid of (34), we can replace the gradient at the wall needed to evaluate the right hand side of Eq. (24). This equation now takes the form

$$\frac{d^2\theta_{s1}}{d\chi^2} = -\phi + \frac{G_0 \theta_{s0}^{3/2}}{\chi^{1/2}} \tag{35}$$

which can be integrated once to give

$$\frac{d\theta_{s1}}{d\chi} = -\int_0^{\chi} \phi \, d\chi + 2G_0 \theta_{s0}^{3/2} \chi^{1/2} + C_0 \ . \tag{36}$$

The values of the constants C_0 and θ_{s0} can now be obtained by imposing the adiabatic boundary conditions (26) at $\chi = 0$ and $\chi = 1$. In particular, we get

$$\theta_{s0} = B = \left(\frac{1}{2G_0} \right)^{2/3} = 1.0824 \tag{37}$$

This expression represents the leading order solution for the temperature of the plate.

Equation (36) can be integrated again, giving the first order correction of the plate temperature

$$\theta_{s1} = -\int_0^{\chi} \int_0^{s} \phi \, ds \, d\chi + \frac{2}{3} \chi^{3/2} + C_1(s) \tag{38}$$

where $C_1(s)$ is to be obtained from the solution of Eqs. (28)–(30) for the fluid, and Eq. (25) for the solid, subjected to the adiabatic boundary condition (26) at both edges. In order to continue with the analysis, we have to specify a form of the normalized heat production function ϕ. We assume, for simplicity, the following power law function

$$\phi = (1+s)\chi^s \tag{39}$$

where the exponent s represents the parameter associated to the distribution of the internal heat source in the strip. Any other function can be included without any difficulty. Therefore, Eq. (38) can be written in the form

$$\theta_{s1} = \sum_{n=0,3/2,s+2} a_n \chi^n \tag{40}$$

where $a_0 = C_1(s)$, $a_{3/2} = 2/3$ and $a_{s+2} = 1/(s+2)$. Equation (28) is linear and to obtain its solution it can be used the principle of superposition. Thus, for a plate temperature of the form

$$\theta_{s1} = \mathrm{A}\chi^n \tag{41}$$

where A is a constant. Then, the function f_1 has the following form:

$$f_1 = \theta_{s0}^{-1/2} \sum_{n=0,3/2,s+2} a_n \chi^n \varphi_n(\xi) \tag{42}$$

where φ_n is the solution of the linear ordinary differential equation

$$\frac{\mathrm{d}^3\varphi_n}{\mathrm{d}\xi^3} + \frac{1}{2} g_0 \frac{\mathrm{d}^2\varphi_n}{\mathrm{d}\xi^2} + \frac{1}{2}\frac{\mathrm{d}^2 g_0}{\mathrm{d}\xi^2}\varphi_n - n\left[\frac{\mathrm{d}g_0}{\mathrm{d}\xi}\frac{\mathrm{d}\varphi_n}{\mathrm{d}\xi} - \frac{\mathrm{d}^2 g_0}{\mathrm{d}\xi^2}\varphi_n\right] = 0 \tag{43}$$

obtained from Eq. (28), with the boundary conditions

$$\varphi_n = \frac{\mathrm{d}\varphi_n}{\mathrm{d}\xi} - 1 = 0 \text{ on } \xi = 0 \quad \text{and} \quad \frac{\mathrm{d}\varphi}{\mathrm{d}\xi} = 0 \text{ as } \xi \to \infty \ . \tag{44}$$

The non-dimensional temperature gradient at the wall can be written as

$$\left.\frac{\mathrm{d}^2\varphi_n}{\mathrm{d}\xi^2}\right|_{\xi=0} = -G_1(n) \tag{45}$$

and its variation with n is shown in Fig. 2. Using the invariance relations, we obtain that $G_1(0) = (3/2)\ G_0 = 0.666$. Therefore, all the terms on the right hand side of Eq. (40) can be accounted for using the above procedure. In this case, the first order temperature gradient at the fluid-plate interface is given by

$$\left.\frac{\partial\theta_1}{\partial\eta}\right|_{\eta=0} = \left.\frac{\partial^2 f_1}{\partial\eta^2}\right|_{\eta=0} = -\theta_{s0}^{1/2} \sum_{n=0,3/2,s+2} a_n \chi^n G_n \tag{46}$$

Substituting this expression into Eq. (25), then integrating it along the plate from $\chi = 0$ to $\chi = 1$, and applying the adiabatic boundary conditions (26) for θ_{s2}, we obtain

$$C_1(s) = \frac{\frac{G_1(s+2)}{(s+2)(s+5/2)} - \frac{1}{3}G_1(3/2)}{2G_1(0)} \ . \tag{47}$$

Summarizing, the non-dimensional temperature of the plate for large values of the parameter α can be written as

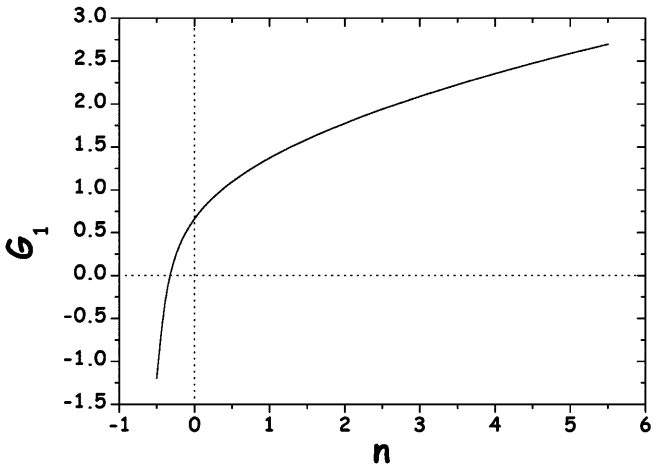

Fig. 2. Variation of the non-dimensional temperature gradient $G_1(n)$ as a function of n

$$\theta_s = 1.0824 + \frac{1}{\alpha}\left(-\frac{1}{s+2}\chi^{s+2} + \frac{2}{3}\chi^{3/2} + C_1(s)\right) + O(\alpha^{-2}) \tag{48}$$

and using the results obtained in this section, the average non-dimensional temperature of the strip is given, up to terms of order α^{-1}, by

$$\bar{\theta}_s = \int_0^1 \theta_s \,\mathrm{d}\chi = 1.0824 + \frac{1}{\alpha}\left(\frac{\frac{G_1(s+2)}{(s+2)(s+5/2)} - \frac{1}{3}G_1(3/2)}{2G_1(0)} + \frac{4}{15} - \frac{1}{(s+2)(s+3)}\right) + O(\alpha^{-2}) \ . \tag{49}$$

Also, the reduced mass flow rate of the fluid, $m_r = m/(\mathrm{Ra}^{*1/3}\rho_f\alpha_f)$, at $\chi = 1$, can be written, up to terms of order α^{-1}, as

$$m_r \simeq \theta_{s0}^{1/2} g_{0\infty} + \frac{\sum_{n=0,3/2,s+2} a_n \varphi_{n\infty}}{\alpha} = 1.6767 + \frac{m_{r1}(s)}{\alpha} \tag{50}$$

where $g_{0\infty} = g_0(\infty)$ and $\varphi_{n\infty} = \varphi_n(\infty)$. The values of $C_1(s)$ and m_{r1} are plotted in Fig. 3 as a function of the parameter s. For the particular case of $s = -1/2$, we have $\theta_s = \theta_{s0} = 1.0824$, which represents the exact solution of the governing equations and is independent of the value of α. The same holds for the reduced mass flow rate $m_r = m_{r0} = 1.6767$, when $s = -1/2$ and any value of α. Due to the fact that m_{r1} is always negative for any value of $s > -1/2$, the mass flow rate decreases as the value of α decreases and the value of s increases.

3.2
Asymptotic limit $\alpha \to 0$

In this case, the longitudinal heat conduction in the strip is very small and can be neglected except in small regions close to the edges of the strip, which only have a local influence. Thus, from Eq. (20) with $\alpha = 0$ and ϕ given by Eq. (39), we have

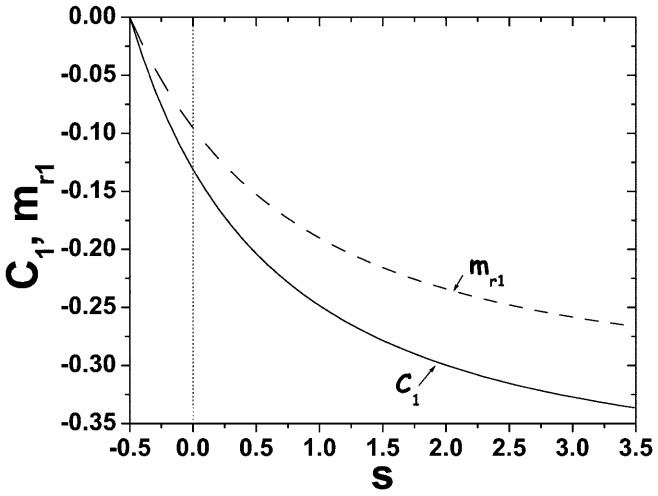

Fig. 3. Variation of the non-dimensional temperature $C_1(s)$ and the reduced mass flow rate $m_{r1}(s)$ at the top of the strip for the case of thermally thin wall regime, as a function of the internal heat distribution parameter s

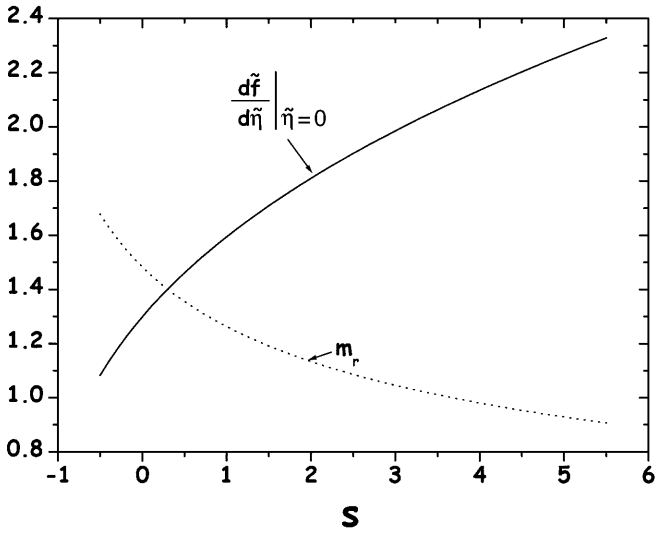

Fig. 4. Variation of $\left.\frac{\mathrm{d}\tilde{f}}{\mathrm{d}\tilde{\eta}}\right|_{\tilde{\eta}=0}$ and the reduced mass flow rate m_r, as a function of the internal heat distribution parameter s for the case of $\alpha = 0$ and thermally thin wall regime

$$\left.\frac{\partial^2 f}{\partial \eta^2}\right|_{\eta=0} = -\phi\chi^{1/2} = -(1+s)\chi^{s+1/2} \quad . \tag{51}$$

This equation, together with the Eqs. (14), (16) and (19), can be solved easily by a similar scheme developed in the foregoing section. Using the following invariance relations of the boundary layer equations

$$\eta = \chi^{-(s+1/2)/3}\tilde{\eta}, \quad f = \chi^{(s+1/2)/3}\tilde{f} \tag{52}$$

the problem reduces to a conventional heat transfer model with a known uniform heat flux distribution at the surface of the strip. Therefore, the non-dimensional temperature of the strip is given by

$$\theta_s = \chi^{(2s+1)/3}\left.\frac{\mathrm{d}\tilde{f}}{\mathrm{d}\tilde{\eta}}\right|_{\tilde{\eta}=0} \tag{53}$$

where $\left.\frac{\mathrm{d}\tilde{f}}{\mathrm{d}\tilde{\eta}}\right|_{\tilde{\eta}=0}$ is to be obtained by solving the nonlinear ordinary differential equation

$$\frac{\mathrm{d}^3\tilde{f}}{\mathrm{d}\tilde{\eta}^3} + \frac{s+2}{3}\tilde{f}\frac{\mathrm{d}^2\tilde{f}}{\mathrm{d}\tilde{\eta}^2} - \frac{(2s+1)}{3}\left(\frac{\mathrm{d}\tilde{f}}{\mathrm{d}\tilde{\eta}}\right)^2 = 0 \tag{54}$$

with the boundary conditions

$$\frac{\mathrm{d}^2\tilde{f}}{\mathrm{d}\tilde{\eta}^2} + (1+s) = \tilde{f} = 0 \quad \text{at } \tilde{\eta} = 0 \tag{55}$$

$$\frac{\mathrm{d}\tilde{f}}{\mathrm{d}\tilde{\eta}} = 0 \quad \text{as } \tilde{\eta} \to \infty \quad . \tag{56}$$

The variation of $\left.\frac{\mathrm{d}\tilde{f}}{\mathrm{d}\tilde{\eta}}\right|_{\tilde{\eta}=0}$ as a function of s is shown in Fig. 4 and it represents the non-dimensional temperature at $\chi = 1$. It means that the maximum temperature at the strip is achieved for increasing values of s. However, the averaged non-dimensional temperature

$$\bar{\theta}_s = \frac{3}{2s+4}\left.\frac{\mathrm{d}\tilde{f}}{\mathrm{d}\tilde{\eta}}\right|_{\tilde{\eta}=0} \tag{57}$$

decreases with s. The reduced mass flow rate at the top of the strip is $m_r(s) = \tilde{f}(\infty)$, and is also plotted in Fig. 4. For the particular case of $s = -1/2$, Eqs. (54)–(56) reduce to Eqs. (27), (29) and (30). The solution of these equations for $s = -1/2$ is clearly $\bar{\theta}_s = 1.0824$. For increasing values of s, the fluid velocity close to the strip increases, but the overall mass flow rate at the top of the strip, decreases.

4 Thermally thick wall regime

In this regime, $(\varepsilon \ll 1)$, the longitudinal heat conduction is also very small and is to be neglected. The energy balance equation (15) for the plate then reduces to

$$\frac{\partial^2\theta_s}{\partial z^2} = -\frac{\varepsilon^2}{\alpha}(1+s)\chi^s \quad . \tag{58}$$

and it has to be solved with the boundary conditions:

$$\begin{aligned} &\frac{\partial\theta_s}{\partial z} = 0 \quad \text{at } z = -1, \\ &\frac{\partial\theta_s}{\partial z} = \frac{\varepsilon^2}{\alpha\chi^{1/2}}\frac{\partial^2 f}{\partial\eta^2} \quad \text{at } \eta = z = 0 \quad . \end{aligned} \tag{59}$$

Integrating Eq. (58) in the normal direction and using the boundary conditions (59), we obtain

$$\left.\frac{\partial^2 f}{\partial\eta^2}\right|_{\eta=0} = -(1+s)\chi^{s+1/2} \tag{60}$$

which is independent of ε and α. The non-dimensional temperature of the plate is then given by

$$\theta_s = \theta_w - \frac{(1+s)\varepsilon^2}{\alpha}\chi^s(z+z^2/2) \qquad (61)$$

where θ_w is the non-dimensional temperature at the lateral surface of the plate in contact with the porous medium, which is given by $\theta_w = \chi^{(2s+1)/3}\frac{d\tilde{f}}{d\tilde{\eta}}\Big|_{\tilde{\eta}=0}$, and is exactly the same as that obtained for the thermally thin wall regime given by Eq. (53). The averaged non-dimensional temperature of the strip is then

$$\bar{\theta}_s = \frac{3}{2s+4}\frac{d\tilde{f}}{d\tilde{\eta}}\Big|_{\tilde{\eta}=0} + \frac{1}{3}\frac{\varepsilon^2}{\alpha} \quad . \qquad (62)$$

In the limit of $\varepsilon^2/\alpha \to 0$, the non-dimensional average temperature of the strip has exactly the same expression than that for the case of $\alpha \to 0$, which is given by Eq. (57). The reduced mass flow rate is also exactly the same as that obtained for the case of $\alpha \to 0$ and thermally thin wall regime.

5 Results and conclusions

For large values of α ($\gg$1) and $s = -1/2$, the average non-dimensional temperature $\bar{\theta}_s$ of the strip reaches the asymptotic value of 1.0824, which corresponds to the case of uniform temperature of the strip, as can be seen from the relation (49). In this asymptotic limit of α, the distribution of the internal heat generation rate does not directly play any important role. The average non-dimensional temperature of the strip decreases for smaller values of α, only controlled by the assumed values of the distribution parameter s. Otherwise, for fixed values of α, we have larger values of $\bar{\theta}_s$ for increasing values of s. These results can be better approximated from Figs. 3 and 4 in order to see the influence of the parameters α and s on the reduced mass flow rate at the top of the strip. In Fig. 3, we have plotted the first order correction for the reduced mass flow rate m_{r1} as a function of the parameter s. Hence, with the aid of the relation (50), we show that for increasing values of α and finite values of s, the reduced mass flow rate decreases. On the other hand, the effect of s for fixed values of α is also to decrease the reduced mass flow rate for larger values of s. Therefore, a convenient way to promote the grow of the reduced mass flow rate, m_r, is to increase the value of α and decrease the distribution parameter s. These results are clearly compatible with previous results for the average temperature of the strip. In the limit $\alpha \to 0$, but holding the thermally thin wall regime ($\alpha/\varepsilon^2 \gg 1$), Fig. 4 shows the non-dimensional wall temperature, θ_w, evaluated at $\chi = 1$ and the reduced mass flow rate, m_r, as functions of the parameter s. It is clear that for decreasing values of s, the reduced mass flow rate, m_r, always increases. Similar comments can easily be made for the average non-dimensional temperature from the relation (57). For the thermally thick wall regime, the above results are identically reproduced if $\varepsilon^2/\alpha \to 0$, as can easily be seen from the relation (62).

The non-dimensional governing equations for the thermally thin wall regime, (14) and (20), were numerically integrated using the quasi-linearization technique for the fluid-saturated porous medium. A quasi-transient term was added to the energy equation of the strip (20). The numerical solution for the averaged temperature of the strip, $\bar{\theta}_s(s,\alpha)/\theta_{s0}$, is plotted in Fig. 5 as a function of α and three different values of s. Here, it is clearly seen how the average temperature of the plate decreases as the value of α decreases and this is in agreement with the results presented in the previous paragraph. It is also seen that the average temperature decreases faster for larger values of the distribution parameter s. Finally, Figs. 6 and 7 show the numerical solution for the non-dimensional temperature of the strip, as a function of the normalized longitudinal coordinate for different values of α. The solution for $\alpha = 0$, given by Eq. (53) is also plotted in these figures, showing an important discrepancy with the numerical solution for $\alpha = 0.001$, especially at the bottom end of the strip ($\chi = 0$) for $s = 0$. However, for $s = 2$, both solutions are almost indistinguished, indicating that the solution obtained for $\alpha = 0$, gives excellent results for small values of α.

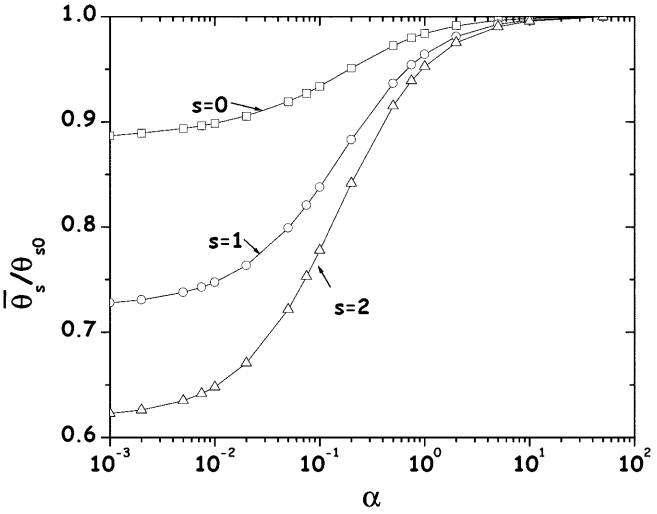

Fig. 5. Numerical solution for the normalized overall temperature of the strip, $\bar{\theta}_s/\theta_{s0}$, as a function of α and different values of s

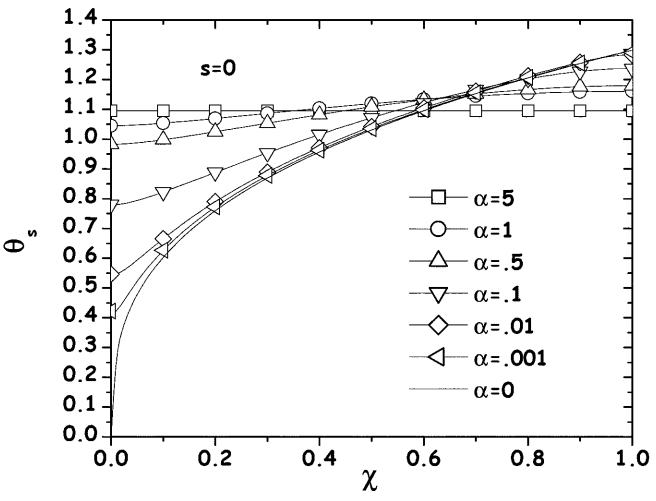

Fig. 6. Numerical solution of the non-dimensional temperature of the strip, $\theta_s(\chi)$, as a function of χ for different values of α and $s = 0$

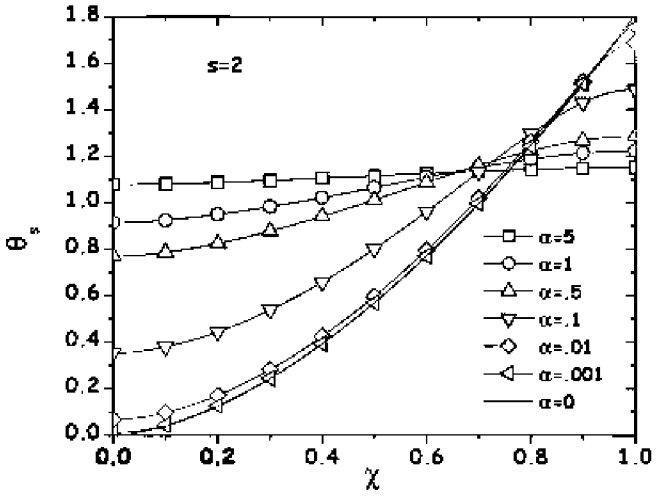

Fig. 7. Numerical solution of the non-dimensional temperature of the strip, $\theta_s(\chi)$, as a function of χ for different values of α and $s = 2$

The conjugated heat transfer process of free convection in a porous medium along a thin strip embedded in a vertical plate has been analyzed for large values of the suitable Rayleigh numbers, using asymptotic as well as numerical techniques. A closed form solution for the temperature of the strip and the mass flow rate have been obtained, covering both the thermally thin and thick wall regimes. Due to the finite thermal conductivity of the strip material and the internal heat generation, the heat transfer by conduction through the strip is a relevant mechanism that can substantially modify the previous estimations of the reduced mass flow rate based on the prescribed boundary conditions. Thus, the free convection along the vertical strip, controlled by the axial heat conduction and the internal heat generation, governs the spatial evolution of the strip's temperature. However, the temperature profiles are controlled by the assumed values of the non-dimensional parameter s related with the distribution of the internal heat source in the solid plate. They can be shown through the average temperatures $\bar{\theta}_s$ given by Eqs. (49), (57) and (62) for the thermally thin and thick wall regimes, respectively. Therefore, the conjugated heat transfer model has a direct influence to restrict the assumed values of the reduced mass flow rates m_r.